

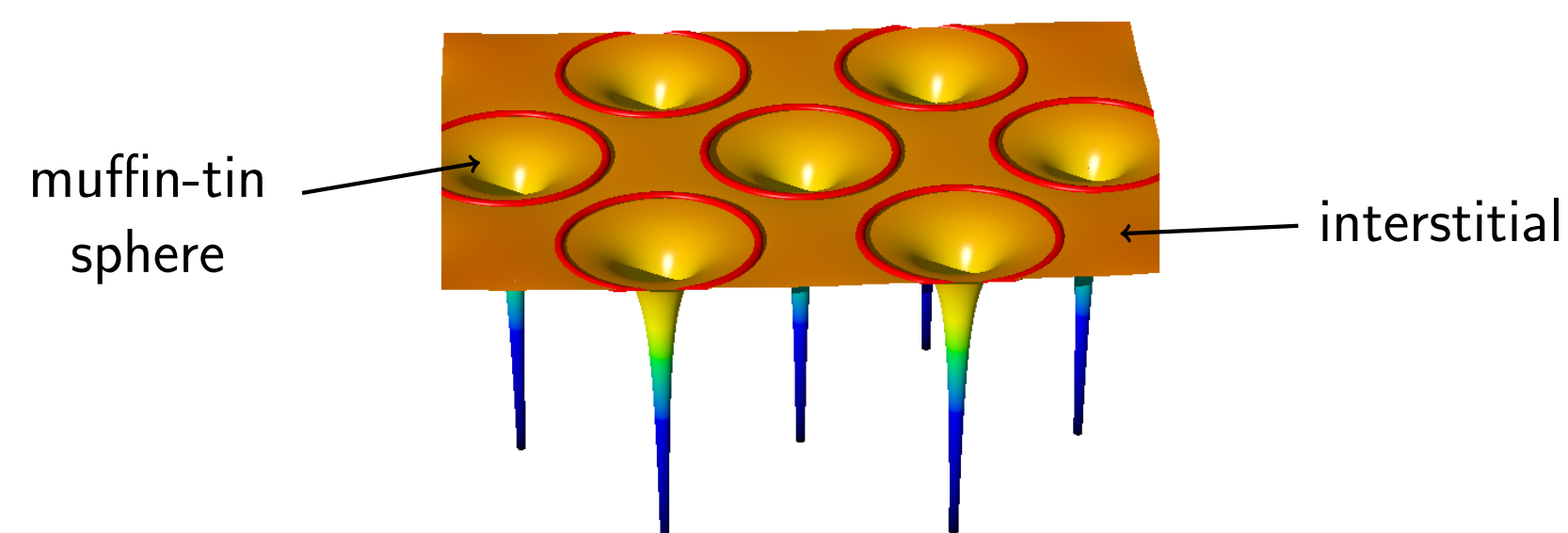
Abstract

The properties of solids are described successfully within density-functional theory. However, the exact exchange-correlation functional is unknown and the commonly used local-density (LDA) and generalized gradient approximation (GGA) fail to predict the band gaps and structural properties of a number of oxide materials. This error is attributed to the self-interaction in LDA and GGA, which is partly corrected in hybrid functionals. Hybrid functionals contain a certain fraction of non-local Hartree-Fock exchange and give excellent agreement with experimental results for oxide materials. We present our implementation of the PBE0 and HSE06 functionals within the all-electron full-potential linearized augmented plane-wave method realized in the FLEUR (www.flapw.de) code [1,2]. We highlight the excellent performance of these functionals for oxide materials, especially for systems in which LDA and GGA predict incorrect properties.

Acknowledgement

We gratefully acknowledge the financial support from the Young Investigators Group Programme of the Helmholtz Association, contract VH-NG-409.

FLAPW Basis



In the FLAPW method space is divided into muffin-tin (MT) spheres and the interstitial region (IR). Within the MT spheres the electronic wave functions are represented by radial numerical functions and spherical harmonics, whereas in the IR a plane-wave representation is used.

$$\chi_{\mathbf{k},\mathbf{G}} = \begin{cases} \frac{1}{\sqrt{N\Omega}} \exp[i(\mathbf{k} + \mathbf{G})\mathbf{r}] & \text{for } \mathbf{r} \in \text{IR} \\ \frac{1}{\sqrt{N}} \sum_{lm} [a_{lm}^{k,\mathbf{G}} u_l(r) + b_{lm}^{k,\mathbf{G}} \tilde{u}_l(r)] Y_{lm}(\hat{\mathbf{r}}) & \text{for } \mathbf{r} \in \text{MT} \end{cases}$$

Hybrid Functionals

In PBE0 hybrid functional [3] non-local Hartree-Fock (HF) exchange replaces a certain fraction of the local PBE GGA exchange.

$$E_x^{\text{PBE0}} = E_x^{\text{PBE}} + a (E_x^{\text{HF}} - E_x^{\text{PBE}})$$

The key difference to the related HSE functional [4,5] is the separation of the Coulomb interaction for the exchange part into a short-range (SR) and a long-range (LR) contribution:

$$\frac{1}{r} = \underbrace{\frac{\text{erfc}(\omega r)}{r}}_{\text{SR}} + \underbrace{\frac{\text{erf}(\omega r)}{r}}_{\text{LR}}$$

In the HSE functional the LR term is approximated by the corresponding LR PBE expression. Thus the exchange energy can be written as

$$E_x^{\text{HSE}} = E_x^{\text{PBE}} + a (E_x^{\text{HF,SR}}(\omega) - E_x^{\text{PBE,SR}}(\omega)),$$

where ω is an adjustable parameter: $\omega \rightarrow 0$ and $\omega \rightarrow \infty$ correspond to the PBE0 and the PBE functional, respectively. It was found [5] that the best agreement with experimental results is achieved for $\omega = 0.11$.

Mixed Basis Ansatz

In a generalized Kohn-Sham the non-local exchange potential is given by

$$V_{\mathbf{x},\mathbf{G}'\mathbf{G}}(\mathbf{k}) = - \sum_{n,q}^{\text{occ.}} \langle \phi_{n,q} | \chi_{\mathbf{k},\mathbf{G}'} | V_{\text{coul}} | \chi_{\mathbf{k},\mathbf{G}} \phi_{n,q} \rangle, \quad (1)$$

where $\phi_{n,q}$ is a Kohn-Sham wavefunction, $\chi_{\mathbf{k},\mathbf{G}}$ and $\chi_{\mathbf{k},\mathbf{G}'}$ are FLAPW basis functions and the sum includes only occupied orbitals.

These matrix elements are needed in each iteration. It is advantageous to introduce a basis for the products $|\phi \chi\rangle$

$$M_{\mathbf{k},I}^{\text{MT}}(\mathbf{r}) = \frac{1}{\sqrt{N}} \sum_{\mathbf{T}_I} U_I(|\mathbf{r} - \mathbf{T}_I|) Y_{L_I M_I}(\widehat{|\mathbf{r} - \mathbf{T}_I|}) e^{i\mathbf{k}\cdot\mathbf{T}_I}$$

$$M_{\mathbf{k},I}^{\text{IR}} = \frac{1}{\sqrt{V}} e^{i(\mathbf{k} + \mathbf{G}_I)\mathbf{r}} \Theta(\mathbf{r} \in \text{IR}).$$

We call this basis *mixed product basis*, because of the mixture of MT and IR basis functions. With the completeness relation for the mixed product basis, we have

$$\langle \phi_{n,q} | \chi_{\mathbf{k},\mathbf{G}'} | V_{\text{coul}} | \chi_{\mathbf{k},\mathbf{G}} \phi_{n,q} \rangle = \sum_{I,J} \langle \phi_{n,q} | \chi_{\mathbf{k},\mathbf{G}'} | \widetilde{M}_{\mathbf{k},I} \rangle \langle \widetilde{M}_{\mathbf{k},I} | V_{\text{coul}} | \widetilde{M}_{\mathbf{k},J} \rangle \langle \widetilde{M}_{\mathbf{k},J} | \chi_{\mathbf{k},\mathbf{G}} \phi_{n,q} \rangle$$

where only the overlap integrals (red) must be evaluated in each iteration step (details in [1]). The matrix $V_{\mathbf{k},I,J}$ (green) is evaluated only once before the self-consistent cycle and stored on hard disc. During the iterations the matrix is loaded and the summation over all mixed basis functions is performed.

Sparse-Matrix Technique: In the construction of the MT functions of the mixed product basis, we have the freedom to construct the radial functions U_I such that all but one function with the same angular moment have a vanishing multipole moment. For all other functions, the matrix $V_{\mathbf{k},I,J}$ vanishes, so that less elements of the overlap integrals have to be calculated. This approach is approximately a factor of 2 faster than an approach not taking care of the multipole moments.

HSE Non-Local Part

For the HSE functional the Coulomb potential in (1) is replaced with an attenuated one

$$V_{\text{coul}}^{\text{att}}(\mathbf{r}, \mathbf{r}') = \frac{\text{erfc}(\omega |\mathbf{r} - \mathbf{r}'|)}{|\mathbf{r} - \mathbf{r}'|}$$

While the Fourier transforms of neither V_{coul} nor $V_{\text{coul}}^{\text{att}}$ converge quickly, their difference does. The Fourier coefficients of the "rest" potential

$$V_{\mathbf{G}}^{\text{rest}} = V_{\text{coul}} - V_{\text{coul}}^{\text{att}} = \frac{\text{erf}(\omega |\mathbf{r} - \mathbf{r}'|)}{|\mathbf{r} - \mathbf{r}'|},$$

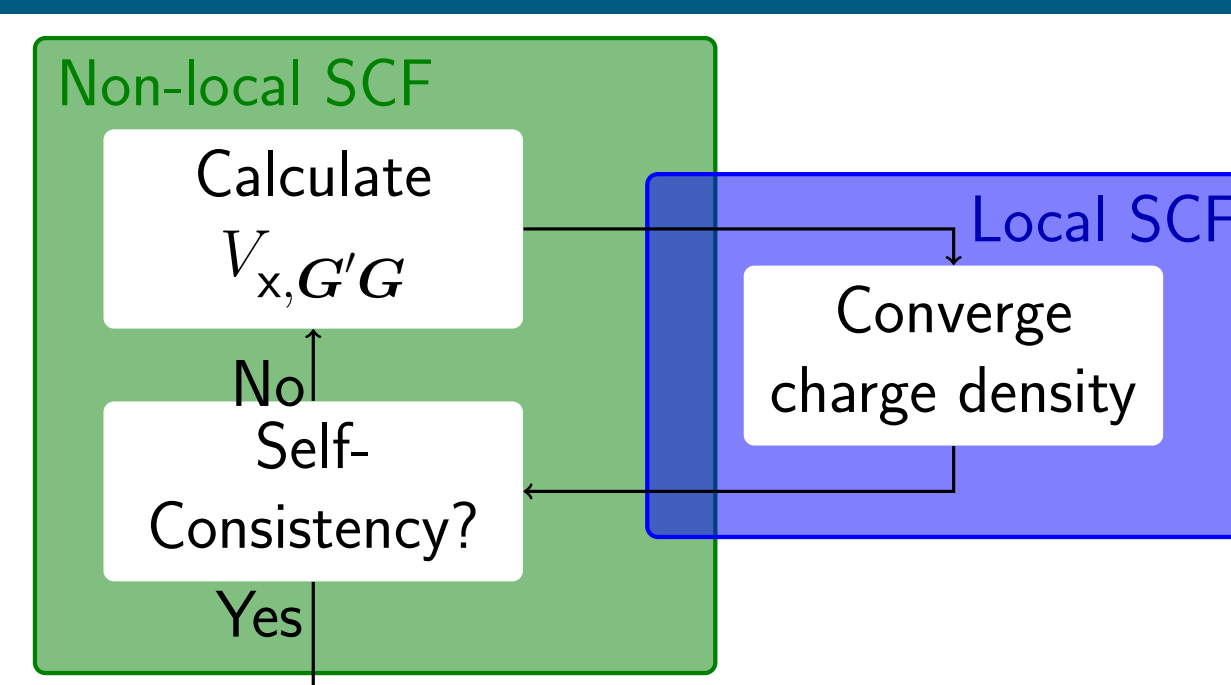
fall off exponentially ($1/4\omega^2 \approx 20$)

$$V_{\mathbf{G}}^{\text{rest}}(\mathbf{k}) = \frac{4\pi}{|\mathbf{k} + \mathbf{G}|^2} \exp\left[-\frac{|\mathbf{k} + \mathbf{G}|^2}{4\omega^2}\right].$$

This allows to evaluate the matrix elements efficiently by a sum over \mathbf{G} vectors

$$\langle M_{\mathbf{k},I} | V_{\text{rest}} | M_{\mathbf{k},J} \rangle = \sum_{\mathbf{G}} \langle M_{\mathbf{k},I} | \mathbf{k} + \mathbf{G} \rangle V_{\mathbf{G}}^{\text{rest}}(\mathbf{k}) \langle \mathbf{k} + \mathbf{G} | M_{\mathbf{k},J} \rangle.$$

Nested Self-Consistency



The most expensive part of the self-consistency is the calculation of the non-local potential $V_{\mathbf{x},\mathbf{G}'\mathbf{G}}$. However, the most change to the total potential during self-consistency originates from the local potential. Thus, an efficient implementation keeps the non-local potential fixed until the local potential is converged. Only then a new non-local potential is calculated.

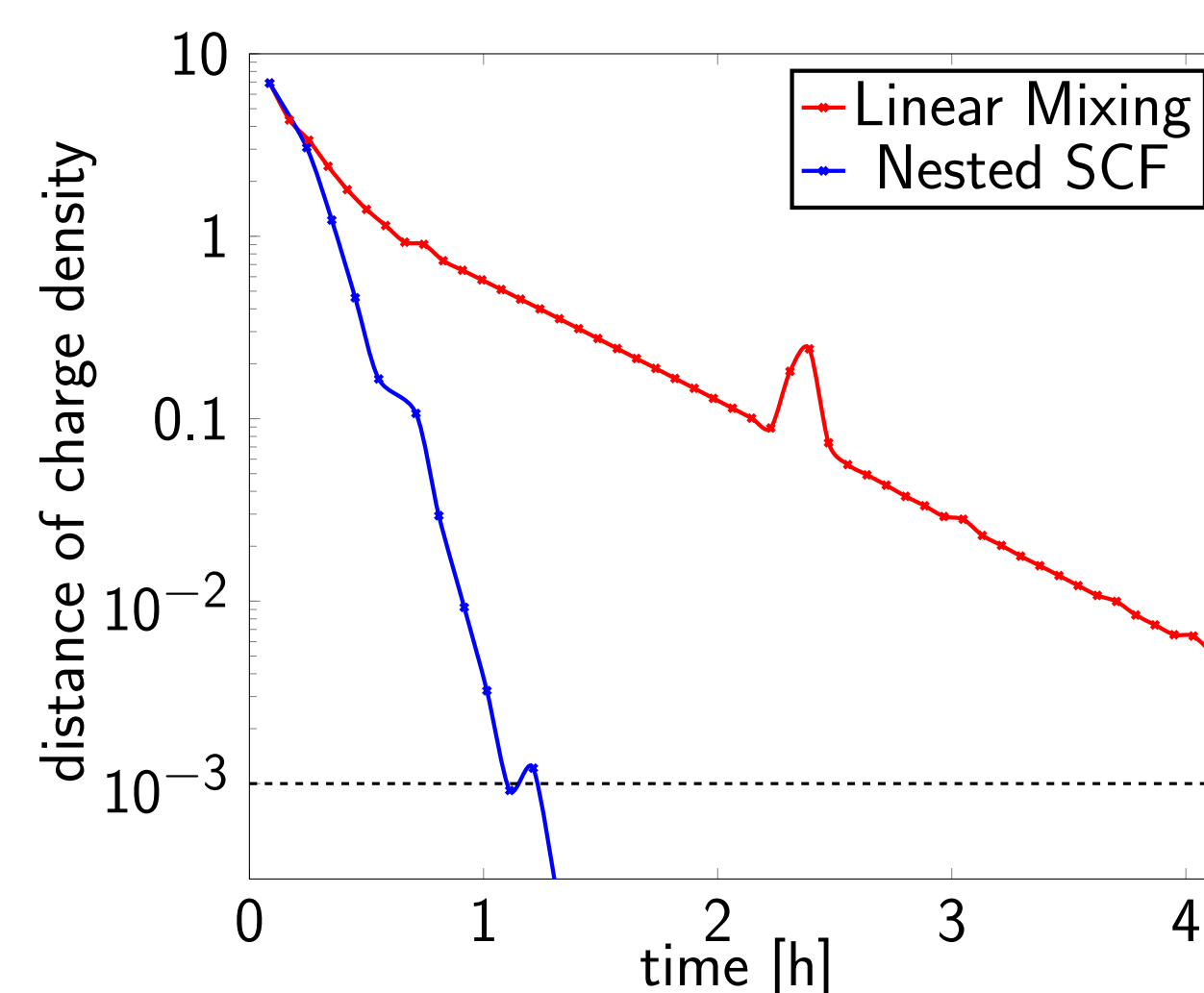


FIGURE: Convergence of charge density for EuO with $6 \times 6 \times 6$ kpt-mesh; drastic improvement of execution time with nested self-consistency (cluster with 8 processors calculation)

Total Energy

The total energy of the system is given as

$$E = \langle T \rangle + E_{\text{eff}} + E_{\text{xc}}$$

The kinetic energy is calculated by a reformulation $T = \mathcal{H} - V$

$$\langle T \rangle = \sum_i \epsilon_i - \langle V_{\text{eff}} \rangle + \langle V_{\text{xc}} \rangle$$

By the hybrid functionals, the expression E_{xc} is altered corresponding to PBE by

$$\Delta E_{\text{xc}} = a \left[\frac{1}{2} \sum_{ij}^{\text{occ.}} \langle \phi_i \phi_j | V_{\text{coul}} | \phi_j \phi_i \rangle - E_x^{\text{PBE}} \right]$$

and the term $\langle V_{\text{xc}} \rangle$ is modified by an additional term

$$\Delta \langle V_{\text{xc}} \rangle = a \left[\sum_{ij}^{\text{occ.}} \langle \phi_i \phi_j | V_{\text{coul}} | \phi_j \phi_i \rangle - \langle V_x^{\text{PBE}} \rangle \right].$$

As we include HF exchange only for valence states, the first summation over i only includes valence states. The second summation over j includes all occupied states.

In HSE, the Coulomb potential is replaced with an attenuated Coulomb potential and only the short-ranged component of the PBE part is taken into account.

k-point Convergence

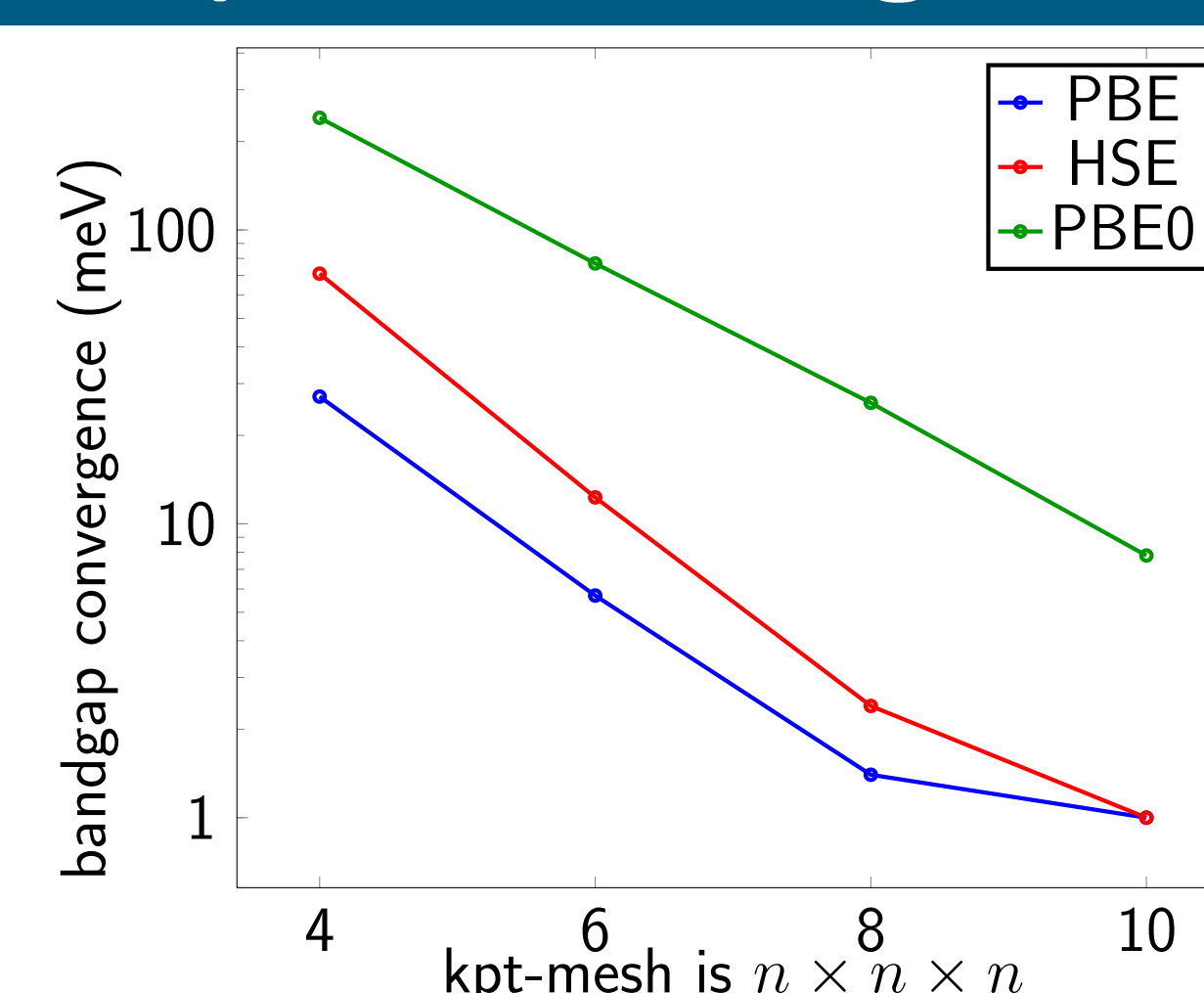
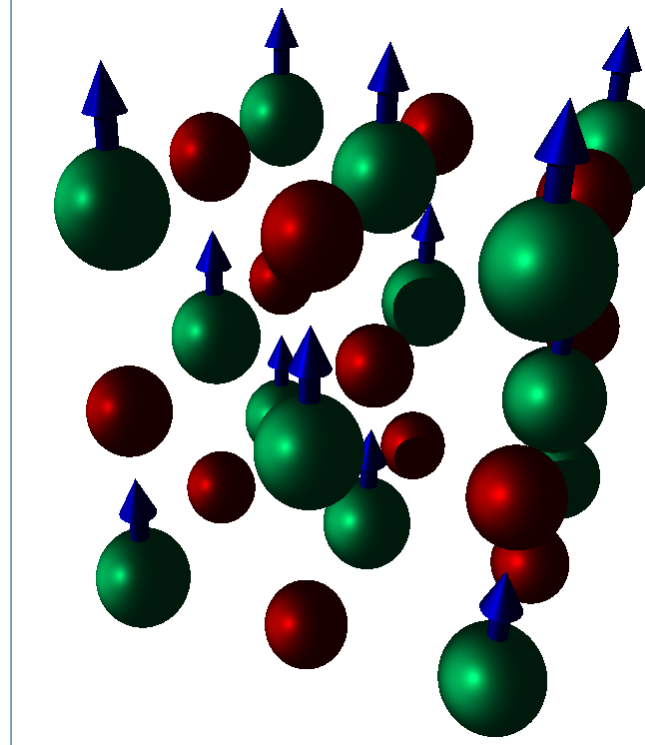


FIGURE: The difference of the bandgap to a converged value ($12 \times 12 \times 12$ mesh) converges much faster in PBE and in HSE than in PBE0.

Rare Earth Compounds

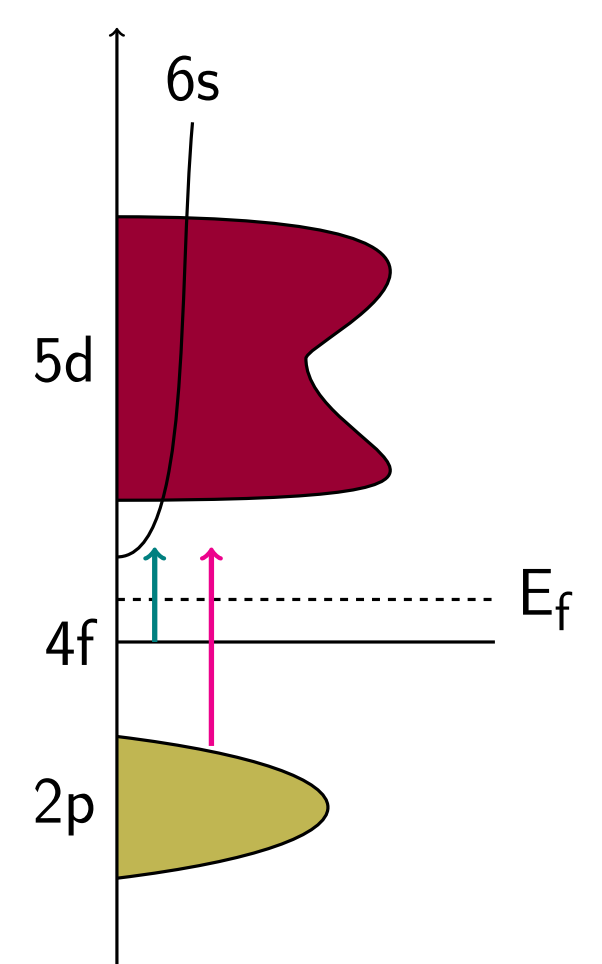


We investigated two rare earth compounds, namely EuO and GdN. These materials are ferromagnetic with an ordering temperature around 60 K. Upon passing the Curie temperature the resistance drops by several orders of magnitude.

Europium Oxide

The right figure shows a schematic density of states (DOS) for the majority spin in europium oxide. The minority spin DOS looks similar only that the 4f-states are above the Fermi energy and thus unoccupied.

With a common exchange correlation functional such as the PBE-GGA, density functional theory cannot predict the experimentally observed DOS (see table below). With the hybrid functionals the position of the 4f-states is corrected, so that the system has a finite bandgap. Furthermore hybrid functionals improve the lattice constant and the bulk modulus.



	GGA	HSE	PBE0	exp.
lattice constant [Å]	5.088	5.141	5.141	5.127 [6]
bulk modulus [GPa]	100.9	94.6	95.4	92 [7]
gap 4f - CB [eV]	-1.3	0.4	1.2	1.1 [8]
gap 2p - CB [eV]	2.5	4.0	4.8	4.1 [9]

Gadolinium Nitride

In a recent work, Larson *et al.* [10] examined the properties of the rare earth nitride series. They used a LSDA+U approach to calculate these materials as the common exchange correlation functionals are insufficient to describe the localized f-states. They tuned the value of U to match the experimental bandgap in GdN.

	GGA	HSE	LSDA+U	exp.
lattice constant [Å]	4.992	4.979	5.08	4.986 [11]
bulk modulus [GPa]	150	160	150	192 [12]
$X \Rightarrow X_{T < T_C}$ [eV]	-0.27	0.50	-	-
$\Gamma \Rightarrow X_{T < T_C}$ [eV]	-0.45	0.02	0.14	-
$X \Rightarrow X_{T > T_C}$ [eV]	0.41	1.19	0.98*	0.98
$\Gamma \Rightarrow X_{T > T_C}$ [eV]	0.35	0.92	0.69	-

LSDA+U results from [10], where U is tuned to match gap *

We compare the results obtained within a HSE calculation with their results and find that one can get a reasonable agreement. Comparing to the experimental results, we improve on the lattice constant. In experiment, the bandgaps are measured above the Curie temperature, so that one has to calculate an approximate bandstructure from the 0K results. In their work, Larson *et al.* proposed to intermix the states of both spins at 0K to get an estimate for the values above T_C . The values in the table above were calculated using the same method for our eigenvalues.

Conclusion

The implementation of the hybrid functionals in the FLAPW method is realized by projecting the products of wavefunction and basisfunction on an auxiliary mixed product basis. This basis consists of functions non-zero only in the MT spheres or the interstitial region and is optimized in the muffin-tin part to calculate as few elements as possible. The HSE functional is implemented via a Fourier transform of the potential difference.

The core states have to be treated separately from the valence states when one calculates the total energy, as the eigenvalues and -vectors of these states are calculated using a simple PBE Hamiltonian.

The execution of the calculation is more efficient by introducing a nested self-consistency scheme as the changes in the non-local potential are much smaller than in the local part.

The HSE functional has a superior kpt-convergence with respect to the PBE0 functional due to its shorter range.

The rare-earth compounds EuO and GdN are described well with hybrid functionals, though the common GGA cannot predict their bandgap. The lattice constants have less than half a percent mismatch compared to the experimental one. Both systems are correctly found to be insulators in hybrid functional calculations.

References

- [1] M. Betzinger, C. Friedrich, and S. Blügel, Phys. Rev. B **81** (2010), 195117
- [2] M. Schlipf, M. Betzinger, M. Ležaić, C. Friedrich, and S. Blügel, in preparation
- [3] J. P. Perdew, M. Ernzerhof, and K. Burke, J. Chem. Phys. **105** (1996), 9982-9985
- [4] J. Heyd, G. E. Scuseria, and M. Ernzerhof, J. Chem. Phys. **118** (2003), 8207-8215
- [5] A. V. Kravau, O. A. Vydrov, A. F. Izmaylov, and G. E. Scuseria, J. Chem. Phys. **125** (2006), 224106
- [6] F. Lvy, Phys. Kondens. Mater. **10** (1969), 71
- [7] Y. Shapira and T. B. Reed, J. Appl. Phys. **40** (1969), 1197
- [8] P. Wachter, CRC Crit. Rev. Solid State Sci. **3** (1972), 189
- [9] D. E. Eastman, Phys. Rev. B **8** (1973), 6027-6029
- [10] P. Larson, W. R. L. Lambrecht, A. Chantis, and M. van Schilfgaarde, Phys. Rev. B **75** (2007), 045114
- [11] G. Busch, P. Junod, O. Vogt, and F. Hulliger, Physics Letters **6** (1963), 79-80
- [12] B. U., J. Alloys Compd. **223** (1995), 216